Pergamon

PII: S0306-4549(96)00004-7

Ann. Nucl. Energy Vol. 23, No. 16, pp. 1271–1287, 1996
Published by Elsevier Science Ltd
Printed in Great Britain

MCNP-DSP: A NEUTRON AND GAMMA RAY MONTE CARLO CALCULATION OF SOURCE-DRIVEN NOISE-MEASURED PARAMETERS†

T. E. VALENTINE and J. T. MIHALCZO
Oak Ridge National Laboratory, P.O. Box 2008, Oak Ridge, TN 37831-6010, U.S.A.

(Received 2 December 1995)

Abstract—The ^{252}Cf-source-driven noise analysis measurement method was developed to determine the subcriticality and other properties of configurations of fissile material. The method provides measured parameters that can also be used for nuclear weapons identification, nuclear materials control and accountability, quality assurance, process monitoring, and verification of calculation models and cross section data used for criticality safety analyses. MCNP-DSP was developed to calculate the measured frequency analysis parameters, time analysis quantities such as autocorrelation and cross-correlation functions, and the time distribution of counts after ^{252}Cf fission for both neutrons and/or gamma rays using continuous energy cross sections. MCNP-DSP can be used to validate calculational methods and cross section data sets with measured data from subcritical experiments. In most cases the frequency analysis parameters are more sensitive to cross section changes by as much as 1 or 2 orders of magnitude and thus may be more useful than comparisons of neutron multiplication factors for calculational validation. The use of MCNP-DSP model in place of point kinetics model to interpret subcritical experiments extends the usefulness of this measurement method to systems with much lower neutron multiplication factors. MCNP-DSP can also be used to determine the calculational bias in the neutron multiplication factor (a quantity which is essential to the criticality safety specialist) from in-plant subcritical experiments. This paper describes how MCNP-DSP calculates the measured parameters from the ^{252}Cf-source-driven time and frequency analysis measurement. Published by Elsevier Science Ltd

1. INTRODUCTION

The subcriticality of configurations of fissile materials is essential for the safe operation of facilities that produce, process, utilize, or store fissile material. Several techniques have been employed to obtain the subcriticality of a given fissile assembly, for example, inverse kinetics (Sastre, 1960), modified source neutron multiplication (Mueller *et al.*, 1962), break frequency noise analysis (Ricker *et al.*, 1963), source jerk (Jankowski *et al.*, 1957), and pulse neutron methods (Simmons and King, 1958). However, these methods have difficulties that have precluded their use for practical in-plant applications. Several of these methods depend on detection efficiency, which may be more sensitive to changes in the geometry of the fissile configuration than to changes in k_{eff}. Many of the methods require a calibration near delayed critical in order to obtain a value for k_{eff}; consequently, this is not practical for in-plant situations where criticality cannot be achieved. Some of these methods also depend on the intensity of the source which can further obscure the determination of k_{eff}. To alleviate these difficulties, the ^{252}Cf source driven method was developed in the time domain to obtain a measured quantity related to $\Delta k/k$ but not related to detection efficiency (Mihalczo, 1971). This measurement evolved from time domain Rossi-α measurements (Orndoff, 1957) and randomly pulsed neutron measurements with ^{252}Cf in ionization chambers (Milhalczo, 1974). The frequency analysis equivalent of these combined time domain measurements was then formulated to exploit the advantages of frequency analysis (Paré and Mihalczo, 1975). The first measurements were performed in 1974 (Mihalczo, *et al.*, 1978). This measurement technique has been proven to be very sensitive to small changes in the

† Research sponsored by the U.S. Department of Energy and performed at Oak Ridge National Laboratory, managed by Lockheed Martin Energy Systems, Inc., for the U.S. Department of Energy under contract DE-AC05-840R21400.

fissile configuration. This sensitivity (in some cases as much as a factor of 50 more sensitive than k_{eff}) has been demonstrated in various subcritical measurements and in Monte Carlo calculations of the measured data (Mihalczo and Valentine, 1995).

This measurement method employs two or more particle detectors along with a ^{252}Cf source to provide measured quantities that can be directly calculated for the verification of calculational methods and cross section data sets and to determine the neutron multiplication factor of a subcritical assembly. The source, which is contained within an ionization chamber, is placed in or near the subcritical fissile configuration to initiate the fission chain multiplication process. For each spontaneous fission of ^{252}Cf an electrical pulse is produced that indicates the time of fission and emission of neutrons and gamma rays. The particle detectors are placed in or near the fissile assembly to measure particles from the fission chains induced by the spontaneous fission of the ^{252}Cf source. To avoid limitations of source intensity and background that must be subtracted in the time domain measurements, frequency analysis measurements analogous to the time domain methods were performed. By combining these measurement techniques into one measurement, a measurement of a subcritical fissile assembly could be performed without dependence on detection efficiency, without dependence on source intensity as long as there are no intrinsic or other significant sources of detected events in the fissile configuration other than the ^{252}Cf source, and without requiring a measurement near delayed critical.

A certain ratio of spectral densities, $R(\omega)$, obtained from the measured data has these properties. The ratio of spectral densities is defined as

$$R(\omega)=\frac{G_{12}^{*}(\omega)G_{13}(\omega)}{G_{11}(\omega)G_{23}(\omega)}, \tag{1}$$

where ω is the angular frequency; G_{12}^{*} is the complex conjugate of the cross-power spectral density (CPSD) of the source detector #1 and detector #2, which detects particles from fission; G_{13} is the CPSD of the source detector #1 and the particle detector #3; G_{11} is the auto-power spectral density (APSD) of the source detector; and G_{23} is the CPSD between the two particle detectors. To avoid the limitation of the point kinetics model, a more generalized particle transport model was developed using Monte Carlo in order to obtain the subcriticality of a fissile assembly by direct calculation of the measured spectral densities. Verification of the Monte Carlo model and the cross sections with noise measured parameters for a particular application establishes the bias in the calculated noise measured parameters. The bias in the noise measured parameters can be translated into a bias in the neutron multiplication factor and be used to infer the neutron multiplication factor from the measured data.

The KENO-NR (Ficaro, 1991) Monte Carlo code was developed by Ficaro from KENO Va (Petrie and Landers, 1984) to calculate the spectral densities of this measurement. However, this code is limited in that it only calculates the detector responses due to neutrons and uses group cross section, whereas the most efficient detectors used in the measurements detect both neutrons and gamma rays. Sometimes gamma ray detectors are used exclusively in the measurements. Because of these limitations, a more generalized Monte Carlo model which has continuous energy cross sections and which also includes gamma rays was needed to calculate the spectral densities.

To provide a more detailed model, the Monte Carlo code MCNP (Briesmeister, 1993) was modified to calculate both the time domain detector responses and the spectral densities from this measurement. Several modifications were made to the neutron and gamma ray tracking routines of MCNP™† such that the calculated parameters are obtained as measured. The structure of the code was modified in order to obtain data blocks of detector responses, as in measurements. The data blocks are time samples of detector response, typically of 512 or 1024 points, for a certain time period which is determined from the sampling rate of the data acquisition system. The particle weighting and biasing in MCNP were disabled in order to have a strictly analog Monte Carlo calculation that follows physically the actual particle random walks. A dual particle source was developed which produces both neutrons and gamma rays from the fission of ^{252}Cf in which the time tracking of the gamma rays was coupled to that of the neutrons. Additional evaluated measured data were incorporated into the code for certain neutron and gamma ray interactions to more precisely follow the physics of particle interaction on an event by event basis. Average quantities like $\bar{\nu}$, the average number of prompt neutrons per fission, were removed from MCNP-DSP because average quantities remove some of the statistical fluctuations from the fission chain populations. Experimental data describing the probability distribution of the number of prompt neutrons from fission were incorporated into the

† ™MCNP is a trademark of the Regents of The University of California, Los Alamos National Laboratory.

code where available; otherwise, the Gaussian theoretical distribution is used. A modified Maxwellian energy distribution was included in the code to obtain the energy of prompt neutrons from the spontaneous fission of ^{252}Cf along with angular distribution data for neutrons from fission to describe anisotropy of the neutron directions in the laboratory system. The energy distribution of gamma rays from the spontaneous fission of ^{252}Cf and the multiplicity of these gamma rays was also incorporated into MCNP-DSP. MCNP-DSP correlates both the neutrons and gamma rays in time after the fission throughout the fission chain multiplication process. However, as in MCNP, the gamma ray production is not directly correlated to the type of neutron event. Several detector options were included in MCNP-DSP to allow calculation of the responses of the various neutron and gamma sensitive detectors used in the measurements. The detectors used in MCNP-DSP are capture detectors, scatter detectors, or fission detectors. A new simplified algorithm for treatment of multiple scattering events in the scatter detectors was included in addition to multiple scattering of particles between detectors. Data processing algorithms were also incorporated into the code to process the detector responses for both time and frequency analysis. The frequency spectra can be obtained by directly calculating the Fourier transforms of N point blocks of pulses from the detectors and performing a complex multiplication to obtain the APSDs and the CPSDs. The APSDs and CPSDs are also obtained by Fourier transforming the auto correlation and cross-correlation functions. The time distribution of detector counts after ^{252}Cf fission is also calculated.

MCNP-DSP is a complete calculation of time and frequency analysis methods without the limitations of KENO-NR. MCNP-DSP provides a more general continuous energy Monte Carlo calculation of measured parameters, which includes not only prompt neutrons but also prompt gamma rays coupled in time with the neutrons. It can be used to interpret subcritical measurements to obtain the neutron multiplication factor and thus replaces limited point kinetics models, thus extending the usefulness of this measurements. MCNP-DSP provides a more general tool for planning and interpreting experiments for criticality safety (Mihalczo *et al.*, 1995a), safeguards, nondestructive assay (Mihalczo *et al.*, 1995b), and arms control verification (Mihalczo and Paré, 1994) and for verification of calculational methods (Mihalczo and Valentine, 1994).

2. NOISE ANALYSIS RELATIONSHIPS

In this section, some basic frequency analysis quantities are defined, and the measurement of the quantities is then discussed. Finally, the basis of the Monte Carlo calculation of this measurement method is presented.

2.1. Frequency analysis measured quantities

In the measurement, detector pulses are sampled as a function of time in order to obtain the various auto and cross-power spectral densities. The auto- and cross-power spectral densities are defined by performing a complex multiplication of the Fourier transform of the blocks of detector signals. The auto power spectral density (APSD) is defined as

$$G_{xx}(\omega) = X^*(\omega)X(\omega), \tag{2}$$

where $X(\omega)$ is the Fourier transform of the detector signal and * denotes the complex conjugate. Similarly, the cross-power spectral density (CPSD) between two signals $x(t)$ and $y(t)$ is defined as

$$G_{xy}(\omega) = X^*(\omega)\,Y(\omega). \tag{3}$$

In the measurement, the detector signals are sampled as blocks of data that are Fourier transformed. A data block is a sample of the detector response for a certain time period which is determined from the sampling rate of the data analysers and the number of time bins per block. The APSDs and CPSDs are averaged over many data blocks to obtain better and better estimates with increasing numbers of data blocks of the APSDs and CPSDs.

The auto- and cross-power spectral densities can also be defined by taking the Fourier transform of the autocorrelation and cross-correlation functions of the detector responses, respectively. The autocorrelation function is defined as

$$\phi_{xx}(\tau) = \lim_{T\to\infty} \frac{1}{2T} \int_{-T}^{T} X(t)X(t+\tau)\,\mathrm{d}t, \tag{4}$$

where $x(t)$ is the detector time response. The autocorrelation function of a variable is the measure of similar information contained in the variable at time t and the correlated information contained in the variable at time $t+\tau$. The APSD is then defined as

$$G_{xx}(\omega) = \int_{-\infty}^{\infty} \phi_{xx}(\tau)\,\mathrm{e}^{-j\omega\tau}\,\mathrm{d}\tau. \tag{5}$$

The cross-correlation function between two signals is defined as

$$\phi_{xy}(\tau)=\lim_{T\to\infty}\frac{1}{2T}\int_{-T}^{T}x(t)y(t+\tau)\,\mathrm{d}t. \tag{6}$$

The cross-correlation function is a measure of the correlated information contained in one signal at time t and the other signal at time $t+\tau$. The CPSD is then defined as

$$G_{xy}(\omega)=\int_{-\infty}^{\infty}\phi_{xy}(\tau)\,\mathrm{e}^{-j\omega\tau}\,\mathrm{d}\tau. \tag{7}$$

The coherence between two signals is the measure of the degree to which one signal depends on the other signal. It is the fraction of information that is common to both signals and varies between 0 and 1. The coherence between the detector 2 and the source detector 1 response is defined as

$$\gamma_{12}^2(\omega)=\frac{|G_{12}(\omega)|^2}{G_{11}(\omega)G_{22}(\omega)}, \tag{8}$$

between detector 3 and the source,

$$\gamma_{13}^2(\omega)=\frac{|G_{13}(\omega)|^2}{G_{11}(\omega)G_{33}(\omega)}, \tag{9}$$

and between both detectors,

$$\gamma_{23}^2(\omega)=\frac{|G_{23}(\omega)|^2}{G_{22}(\omega)G_{33}(\omega)}. \tag{10}$$

The following ratio of coherences is equal to the magnitude of the ratio of spectral densities [equation (1)],

$$R(\omega)=\sqrt{\frac{\gamma_{12}^2(\omega)\gamma_{13}^2(\omega)}{\gamma_{23}^2(\omega)}}. \tag{11}$$

Expressing the ratio in the form of coherences, the variance of the ratio can be determined by using the variances of the coherences. Since the coherences are real variables, the estimation of the variance in the ratio is made easier than using the variances of the ratio of spectral densities since some of the CPSDs are complex numbers.

The measured coherences are known to be biased, but they converge to their "true" values. The true coherence between two signals (γ^2) is

$$\gamma^2=\left(\frac{S/N}{1+S/N}\right)^2, \tag{12}$$

where S/N is the signal-to-noise ratio and is assumed to be the same for both signals. King (1980) has shown that the measured coherence ($\hat{\gamma}^2$) satisfies the relation

$$\hat{\gamma}^2=\gamma^2+\frac{(1-\gamma^2)^2}{n}, \tag{13}$$

where n is the number of data blocks. For n equal to one, this relationship is not true unless γ^2 is either zero or one. The measured standard deviation was shown by King to be

$$\sigma_{\hat{\gamma}^2}=\frac{\hat{\gamma}^2(1-\gamma^2)}{\sqrt{1+n\gamma^2/2}}. \tag{14}$$

Since the bias in the coherence, $\hat{\gamma}^2-\gamma^2$, diminishes as $1/n$, the coherences can be used to estimate the amount of data needed for the measured coherence to converge to the true coherence. The bias in the coherence is known precisely and can be removed from the data. For the purpose of error analysis, King has shown that treating the coherences as independent quantities yields a correct estimate of the uncertainty. The fractional error of the ratio is

$$\epsilon_R=\frac{\sigma_R^2}{R}=\frac{[\epsilon_{\hat{\gamma}12}^2+\epsilon_{\hat{\gamma}13}^2+\epsilon_{\hat{\gamma}23}^2]^{1/2}}{2}, \tag{15}$$

where

$$\epsilon_{\hat{\gamma}^2}\approx\frac{\sigma_{\hat{\gamma}^2}}{\hat{\gamma}^2}=\frac{(1-\gamma^2)}{\sqrt{1+n\gamma^2/2}}. \tag{16}$$

2.2. *^{252}Cf-source-driven noise analysis measurement*

As previously mentioned, this measurement employs a ^{252}Cf source and two or more particle detectors. The detector signals after amplification are input to discriminators which are used to eliminate unwanted detector pulses. There are two ways in which the detector pulses may be processed. The first involves directly calculating the frequency spectra of the detector responses to obtain the various APSDs and CPSDs. The second method involves the calculation of correlation functions and then calculating the frequency spectra.

In the first method, the signal pulses from the discriminator are input into a circuit that converts them into voltage pulses that have a constant area and a frequency spectrum defined by an adjustable RC time constant. The signals are then passed through a low-pass filter, which eliminates the upper frequency components that are greater than half the sampling rate. This prevents aliasing from occurring during the discrete Fourier processing of the signals. Aliasing is the folding of high frequencies over to the low frequency when the sampling rate is less than twice

the maximum frequency of the signal. The filtered signal is digitized repeatedly by an analog-to-digital converter to provide an integer value proportional to the voltage of the signal. The digitized data are divided into segments, termed data blocks, of typically 512 or 1024 points, and then the data are Fourier transformed. The APSDs and CPSDs are calculated for each data block by complex multiplication of the transformed data. The latest estimates are then averaged with the previous data to obtain the current APSDs and CPSDs. This process is continued until the desired convergence is reached.

The second method is to calculate the correlation functions from the digitized data. The correlation functions are calculated for each data block and averaged. After all data blocks have been calculated, the average correlation functions are Fourier transformed to obtain the average APSDs and CPSDs. After obtaining the average APSDs and CPSDs, the coherences and the ratio of spectral densities are calculated. Both methods of obtaining the frequency spectra are implemented in this work, since they are independent and can be used to partially verify the calculation method since they provide two different ways of calculating the APSDs and CPSDs.

2.3. *Monte Carlo calculation*

To obtain the neutron multiplication factor from the measured frequency spectra, a model has to be used. The Monte Carlo calculation of this method was developed because of the limitations required in using point kinetics models for interpretation of the measured data. To avoid the limitations of the point kinetics models, the Monte Carlo model is used to calculate the frequency analysis parameters and then to obtain the neutron multiplication factor. The Monte Carlo model does not impose any limitations on the spatial dependence of the calculation. The only limitation on the energy dependence is that imposed by the ENDF cross section data files and other nuclear data such as the representation of the neutron and gamma ray energy spectra from fission.

The detector responses are the supposition of contributions of many fission chain multiplication processes, each initiated by source fission. Monte Carlo is the logical choice to provide a calculation of these measurements since the measurement technique accumulates the contribution of the individual fission chains to the detector responses. In the calculation, fission chains are initiated by ^{252}Cf fission or 14 MeV source. These particles are transported throughout the system. The collision events and sites are probabilistically determined. The production of secondary particles from fission is chosen from the ratio of the fission cross section to the total cross section. These subsequent particles are transported in the same manner as the source particles. When the particles have an event in the detection media, which is specified in the input, a test is performed to determine if the particle contributes to the detector response. The detector responses from each fission chain are superimposed into data blocks consistent with a specified Cf source fission rate. After the necessary blocks of data are obtained, the frequency spectra are calculated.

3. THE MODIFIED MCNP CODE

3.1. *General description of MCNP*

MCNP is a multipurpose Monte Carlo code that is used for neutron, gamma ray, and electron transport. MCNP has a wide array of capabilities, for example, detector tally calculations, flux estimation tallies, and eigenvalue calculations for fissile assemblies. The source can be described in great detail. The source particle type, energy, position, and direction can easily be specified. There are also many variance reduction techniques that can be used if needed.

The code uses a generalized geometry package that allows explicit modeling of a given geometry. The geometry is assembled as cells by defining the surfaces of the unit. The materials that comprise the cells are described using the appropriate material densities along with a descriptor that indicates the cross-section data set to be used in the calculation. These cross sections can either be point-wise data or multigroup data if comparison to other codes is required. The cross-section data sets for neutrons contain all the reactions which have been evaluated for a particular isotope along with any known angular distributions. Cross-section data in the form of thermal $S(\alpha, \beta)$ tables are also available to account for molecular binding effects in scattering of low-energy neutrons. Secondary gamma ray production data are also available in some evaluated data sets. For gamma rays, the code uses cross-section data for incoherent scattering, coherent scattering, the photoelectric effect, and pair production. A continuous slowing-down model is used for the electron transport (Briesmeister, 1993).

3.2. *Modified neutron transport*

Although MCNP is very versatile, several changes were made to the code in order to provide an accurate estimation of the time- and frequency-analysis

parameters. A dual-particle source was developed which produced both time correlated neutrons and gamma rays. The variance reduction features were disabled in order to have strictly analog particle tracking, and the neutron and gamma ray transport routines were modified to better represent the collision physics on an event by event basis. Some simplified detector options were incorporated in MCNP-DSP to represent the detectors used in the measurements. Various processing routines were included in MCNP-DSP to obtain the desired time distributions, correlation functions, or frequency spectra from the data blocks of counts in the detectors.

Since this method measures the behavior of the individual fission chains in a fissile configuration, it is necessary that the calculation be able to adequately simulate the behavior of the individual fission chains. This requires replacing average parameters such as $\bar{\nu}$ with probability distributions because the spectral densities provide statistical estimates of the fission chain fluctuations and the average quantities reduce the fission chain fluctuations. The proper treatment of the angular distribution of neutrons from fission was also included in the calculation to adequately describe the particle direction from fission for both spontaneous fission and induced fission. The selection of the energy of the neutrons from the spontaneous fission of ^{252}Cf has been modified to incorporate recent improvements in the representation of the prompt neutron energy spectrum. Implementing these changes along with analog neutron tracking allow for the more physical representation of the individual fission chains.

3.2.1. Number of prompt neutrons from fission. The probability of obtaining prompt neutrons from fission, $P(\nu)$, for various fissioning isotopes was functionally described by Terrell (1959). Terrell suggested that the neutron multiplicities are dependent on the fission fragment properties. If a Gaussian distribution of the fission fragment excitation energies is assumed, the cumulative probability of observing ν prompt neutrons from fission is approximated as

$$\sum_{n=0}^{\nu} P(n) = \frac{1}{\sqrt{2\pi}} \int_{-\infty}^{(\nu-\bar{\nu}+1/2+b)/\sigma} e^{-1/2t^2}\, dt, \qquad (18)$$

where b is a small correction factor ($<10^{-2}$) to ensure that the νs are positive and σ is the root-mean-square width of the initial total excitation-energy distribution ($\sigma = 1.08$). Terrell has shown that this distribution function can be used to describe the emission probability for several different fissioning isotopes. In MCNP, the $\bar{\nu}$ obtained from the cross-section data sets is a function of the energy of the neutron that induces the fission. Thus the emission probability that was incorporated into MCNP-DSP is an energy dependent distribution. The Gaussian distribution is an approximation to describe the prompt neutron emission probabilities at all energies and is used unless additional measured distribution data tables are included for certain isotopes when available.

An option has been incorporated into MCNP-DSP to use the measured data summarized by Zucker and Holden (1986). Zucker and Holden tabulated the $P(\nu)$ distributions for ^{235}U, ^{238}U, and ^{239}Pu as a function of the energy of the neutron that induces the fission. These tabulated data of Zucker and Holden are used by default. The probability distribution data were fit with least-square polynomials to obtain a functional representation of the energy dependence of neutron emission probabilities. The probability distribution data for the spontaneous fission of ^{252}Cf were taken from Spencer's measurements (Spencer *et al.*, 1982).

3.2.2. Angular distribution of prompt neutrons from fission. There are instances in which the angular distributions of prompt neutrons from fission may be important, such as when the ^{252}Cf source is located some distance from the fissile configuration or perhaps with interacting arrays. Hence, assuming an isotropic emission of neutrons from fission can be a poor approximation. The angular distribution of neutrons relative to the direction of the light fission fragment has been measured by Budtz-Jorgensen and Knitter (1988) for the spontaneous fission of ^{252}Cf. Budtz-Jorgensen and Knitter have shown that there is angular anisotropy in the laboratory reference frame. The probability distribution function obtained from the Budtz-Jorgensen and Knitter data is shown in Fig. 1. As can be seen from Fig. 1, the angular distribution at zero energy is more isotropic; however, as the neutron energy increases, the angular distribution becomes very anisotropic.

These data are incorporated into MCNP-DSP by selecting the direction of the light fission fragment from an isotropic distribution. The neutron direction is then determined by sampling its azimuthal direction uniformly on the interval 0 to 2π. The polar angle of each fission neutron relative to the light fission fragment is determined from the angular probability distribution function. These data may be used for both the spontaneous fission of the ^{252}Cf source and for induced fissions in the system to investigate the effects of the angular dependence of the neutron emission. Since the majority of the neutrons are released from the fully accelerated fission fragments, the angular distribution of the neutrons relative to the direction of the fission fragments is dependent on the deexcitation of the fission fragments. Therefore,

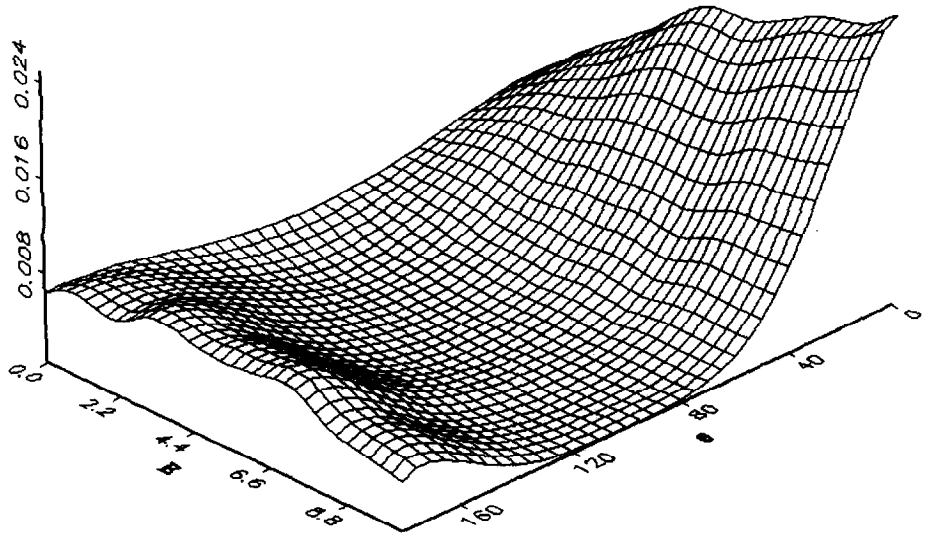

Fig. 1.

there would be little difference between the angular distribution of spontaneous fission neutrons and the angular distribution of induced fission neutrons for fissile isotopes. For these reasons the data for ^{252}Cf was used for all fission (Nix, 1994).

3.2.3. Fission neutron energy distribution for ^{252}Cf. A detailed analysis of the experimental data has been performed by Mannhart (1987) to obtain the relative difference between the neutron spectrum obtained from the measured data and the Maxwellian distribution for the spontaneous fission of ^{252}Cf. Mannhart developed an energy dependent correction factor for the Maxwellian distribution. By multiplying the Maxwellian distribution by the correction factor, an accurate representation of the energy distribution of neutrons from the spontaneous fission of ^{252}Cf is obtained. The average energy obtained from the corrected distribution is 2.13 MeV which corresponds to the measured value of the average energy of neutrons from the spontaneous fission of ^{252}Cf. An eight-point Gaussian quadrature integration scheme was used to integrate the spectrum from zero to an upper limit of E where E was varied from 0.00001 eV to 25 MeV. The integrated spectrum was then normalized to unity. The selection of the neutron energy is determined by setting a random number equal to the normalized integrated spectrum and then determining the energy that corresponds to this value of the normalized integrated spectrum. A least-squares polynomial fit of the neutron energy as a function of the value of the normalized integrated spectrum was used. This resulted in an expression for the neutron energy as a function of the normalized integrated spectrum, that is, the neutron energy as a function of the random number.

3.3. Modified gamma ray transport

In MCNP, gamma ray production from neutron events is determined by sampling a total gamma ray production cross section. These cross sections contain data on the multiplicity and energy of gamma rays from neutron reactions that produce gamma rays. These reactions include neutron capture, inelastic neutron scattering, and fission. Although the cross sections are measured separately, these gamma ray-producing reactions are lumped together in the evaluated nuclear data sets in ENDF. Consequently, these data cannot be easily separated without modifying the ENDF data files. This grouping does not allow the physics of gamma ray production process to be exact on an event-by-event basis but does give a correct average behavior (Seamon, 1994). This will lead to no uncertainty in the first moment of the populations but may introduce some uncertainty into the second moment on which noise-measured parameters depend, especially when inelastic neutron scattering and fission are equally probable. This may also reduce some of the fluctuating phenomena associated with gamma ray production. The multiplicity and energy distribution of prompt gamma rays from the spontaneous fission of the ^{252}Cf source has been included in MCNP-DSP.

3.3.1. Prompt gamma ray multiplicity for ^{252}Cf. The gamma ray multiplicity, like the neutron multiplicity,

is a function of the fission fragment mass but has little dependence on the energy of the neutron inducing the fission. A sawtooth dependence of the gamma ray yield on fragment mass has been observed for the spontaneous fission of ^{252}Cf and for thermal neutron fission of ^{235}U (Vandenbosch and Huizenga, 1973). Since the number of gamma rays emitted is mainly dependent on the fission fragment properties, a single distribution can be used to describe the gamma ray multiplicity for ^{252}Cf.

The gamma ray multiplicity was determined using Brunson's (1982) measurements, which fitted the data to a double Poisson model. Brunson's model depends on the minimum energy of the gamma rays emitted. For a minimum energy of 85 keV, the resulting probability distribution is used to obtain the gamma ray multiplicity

$$\Gamma(G)=0.682\,\frac{7.20^{G}\,e^{-7.20}}{G!}+0.381\,\frac{10.71^{G}\,e^{-10.72}}{G!} \qquad (18)$$

where G is the gamma ray multiplicity. The gamma ray multiplicity ranges from 0 to 20 gamma rays per fission with an average value of 7.79 gamma rays per fission. This value does not differ greatly from that obtained by others (Wagemans, 1991).

3.3.2. Prompt gamma ray energy distribution for ^{252}Cf. The gamma ray energy spectrum has been measured for the spontaneous fission of ^{252}Cf and the thermal-neutron-induced fission of ^{235}U. There appears to be little difference between the spectrum from ^{252}Cf and that from ^{235}U (Wagemans, 1991). Because of the small difference between the two spectra and because the measurements of the ^{235}U gamma ray spectra are more precise, the gamma ray spectra from the thermal neutron fissioning of ^{235}U is used to obtain the gamma ray energy.

The energy spectrum of the prompt fission gamma rays is obtained from the Maienschein's measurements (Maienschein *et al.*, 1958; Goldstein, 1959). From 0.3 to 1 MeV, the distribution is described as

$$N(E)=26.6\,e^{-2.30E}. \qquad (19)$$

In the interval 1.0–8.0 MeV, the distribution is described as

$$N(E)=8.0\,e^{-1.10E}. \qquad (20)$$

The upper energy limit of 8 MeV was selected because nuclear excitation above 8 MeV typically leads to neutron rather than gamma emission. Although Maienschein's experiment determined the gamma ray spectrum down to 0.25 MeV, there are several gamma ray energies that show preferential emission for low multiplicities below 0.3 MeV (Brunson, 1982). On the advice of Ray Nix (1994), the spectrum below 0.3 MeV is represented as

$$N(E)=38.13(E-0.085)\,e^{1.648E}. \qquad (21)$$

The minimum gamma ray energy of 0.085 MeV coincides with Brunson's measurements. Below this energy, gamma ray emission is due to K-shell x-rays from the fission fragments that occur later than the prompt gamma emission from fission. Using this functional representation of the prompt fission gamma ray energy spectrum, a value of 0.898 MeV is obtained for the average gamma ray energy per fission. This value agrees well with the accepted value of 0.88 MeV per fission (Brunson, 1982).

Some correlation exists between the total gamma ray energy release and the number of neutrons emitted from fission. Nifenecker (Nifenecker *et al.*, 1972) has observed that there is competition in the deexcitation mechanism of the fission fragments. This can be expected since it has been shown that the angular momentum of the fission fragments is transferred to the gamma rays and essentially no angular momentum is given to the neutrons as a consequence of selection rules (Vandenbosch and Huizenga, 1973). Nifenecker obtained the following linear relationship between the number of neutrons emitted from fission, ν, and the total gamma ray energy, E_t:

$$E_t=0.75\nu+4. \qquad (22)$$

This relationship can be used to put a limit on the total gamma ray energy from the spontaneous fission of ^{252}Cf source and also couples the gamma ray production with the neutron production.

3.4. The detection process

Although MCNP is capable of tracking electrons, the electron production and subsequent light production in the detectors were not treated rigorously. An intuitive approach was used to determine when particles contribute to the detector response. This approximation faithfully reproduces the measured detector responses. Currently, three detector types can be employed in a calculation: capture, scatter, or fission detectors.

3.4.1. Neutron detection. In the MCNP-DSP calculation, neutron detection is characterized by a particular neutron event. The detector response of capture detectors is primarily due to the absorption of a neutron with the subsequent emission of secondary charged particles, which ionize the detection media and produce an electronic pulse proportional to the kinetic energy of the secondary charged particle. These detectors typically have a very large thermal neutron absorption cross section and a very small scattering

cross section. In MCNP-DSP, if a neutron is absorbed in a capture detector, a count is scored in the appropriate time bin, and the number of detections is incremented.

Scattering detectors are those in which the response is due primarily to neutron scattering in the detection media. To observe a count in a scattering detector, the neutron must transfer a certain preselected amount of energy to the detection material via the kinetic energy of the recoil nucleus, which excites electrons in the scintillation material which produce light that is converted into an electrical pulse by a photomultiplier tube. Although MCNP can handle this scintillation process directly, an intuitive approximation was utilized which assumes that the light production is proportional to the energy deposited by the neutron. An energy threshold is specified in the calculation for each detector. Since multiple neutron scattering can occur in the detector, special attention was given to modeling the multiple scattering in these detectors by specifying a time width, the pulse generation time, in which energy contributions from the events are summed together. If a neutron scatters in the detector and deposits an amount of energy greater than the neutron threshold, a count is registered and additional neutron scatters within the specified pulse generation time of the detector are ignored. However, if the amount of energy deposited in the detector is less than the neutron threshold, the energy of the subsequent neutron scatters in the detector are added together for those events that occur within the pulse generation time of the detector. In order to account for neutrons that may scatter between adjacent detectors several times, the time at which the neutron had its last scattering event in each detector is stored for each neutron track.

In fission detectors, the fission fragments travel through the detection media, ionizing the atoms in the detector. The large energy release per fission allows for easy discrimination of other events that may also produce ionized atoms in the detector. In the calculation, a count is registered each time a fission occurs in the detection media, and the fission neutrons are stored for tracking. The fission detectors may be used for other applications of interest such as time and frequency analysis studies.

3.4.2. Gamma ray detection. Various gamma ray events may lead to a detection in the capture and scattering detectors since the gamma ray events also produce secondary charged particles. If the gamma ray energy deposited is above a certain threshold, which is specified as input to the calculation, gamma ray absorption due to the photoelectric effect can lead to a detection. Likewise, if the gamma ray has an incoherent scatter in the detector and the recoil electron has an energy greater than the threshold, a detection will occur. Multiple scattering of gamma rays in the detector media is treated much in the same way as for neutrons.

3.5. Detector response processing

As previously mentioned in the measurement and in these calculations, the detector responses are sampled into segments call data blocks of typically 512 or 1024 points. In the calculation, the number of ^{252}Cf fissions to occur within a data block is specified. The relationship between the actual ^{252}Cf source and the simulated source is described in Section 3.6.

3.5.1. Direct Fourier processing. In the measurements, the power spectral densities are obtained by Fourier transforming the blocks of processed detector signals and performing a complex multiplication. Prior to sampling into data block the detector signals are input to a bandpass filter to prevent aliasing. To simulate the band pass filter, two filter options can be employed in the calculation. A Rockland and a Precision filter were used in the measurements; hence, functions that represent these filters may be used in the calculations. The upper frequency cutoff is set equal to 40% of the sampling rate as implemented in the measurement to prevent aliasing. These filter functions are only applicable for sampling rates less than 200 kHz since the low pass filter has not been included in the model and its time response affects the detector response for sampling rates greater than 200 kHz. Other higher frequency filter functions could easily be incorporated into the code if the waveforms are available. The time when a particle is detected is determined by adding its time of birth to the time that the particle spent in the system before being detected. A count is registered in the appropriate time bin in the data block. The width of each time bin is determined from the inverse of the sampling rate. Therefore, the time length of the data block is equal to the number of time bins multiplied by the width of the time bins. If the filter functions are employed for each particle detection, the detector pulse is spread out over $\sim$10 time bins (Ficaro, 1991). This is accomplished by placing the digitized values of the normalized filter function which occur at the right boundary of the time bin in the time bins. If the particle detection occurs near the end of the data block, the digitized values in time bins beyond the length of the data block are ignored. Experimentally, the low-frequency components of the detector signal are eliminated by a.c. coupling (high pass filtering). To simulate the implementation of a highpass filter, the average counts per bin are subtracted for each

detector's time spectrum for each data block. The removal of the mean value is performed independently of the implementation of the low-pass filter. There are three commonly used windows that may be employed in the calculation. These windows are the Bartlett, Hanning, and Hamming windows (Oppenheim and Schafer, 1989). These windows are applied to the time spectra to correct for errors due to the finite length of the data block which coincides with a finite length Fourier transform. A Hanning window has been used in the measurements. A fast Fourier transform is applied to the data block. Using the Fourier transform of the data blocks, the APSDs and CPSDs are calculated for each data block and averaged with the values from the previous data blocks. The coherences and the ratio of spectral densities can be calculated using the average APSDs and CPSDs. The data blocks are continuously sampled until the desired convergence criteria are satisfied (King, 1980).

3.5.2. Correlation function analysis. The calculation of the autocorrelation and cross-correlation functions were included in the code. The code calculates circular correlation functions from the detector time response since this is equivalent to performing the complex multiplication in the frequency domain (Oppenheim and Schafer, 1989). The estimate of the circular autocorrelation function is given by

$$R_{xx}(r)=\sum_{k=0}^{N-1} x_k x_{(N-(r-k))}, \tag{23}$$

where x is the detector signal, r is the lag index, and N is the number of points per data block. The detector signal is assumed to be periodic ($x_k=x_{(N+k)}$) because the circular correlation function is calculated. Likewise, the estimate of the circular cross-correlation function is given by

$$R_{xy}(r)=\sum_{k=0}^{N-1} x_k y_{(N-(r-k))}, \tag{24}$$

where x and y are two different detector signals. Average values of the autocorrelation and cross-correlation functions are calculated as the data blocks are updated. The one-sided auto-power spectral density is defined as (Uhrig, 1970)

$$G_{xx}(\omega)=4\int_0^{\infty} R_{xx}(\tau)\cos(\omega\tau)\,\mathrm{d}\tau, \tag{25}$$

for $0<\omega\leqslant\infty$. This result is obtained because the autocorrelation function is symmetric. Since the code produces estimates of the correlation function at discrete lag times, the autocorrelation function can be expressed as a sequence of discrete samples

$$R_{xx}(\tau)=\sum_{k=0}^{N-1} R_{xx}^k\delta(\tau-k\Delta), \tag{26}$$

where Δ is the sampling interval. Substitution of the sequence into equation (26) yields

$$G_{xx}(\omega)=4\int_0^{N\Delta}\sum_{k=0}^{N-1} R_{xx}^k\delta(\tau-k\Delta)\cos(\omega\tau)\,\mathrm{d}\tau, \tag{27}$$

where the upper limit of the integral has been set equal to $N\Delta$ since this is the period of the data block. Interchanging the order of summation and integration and evaluation of the integral yields

$$G_{xx}(\omega)=4\left[R_{xx}^0+\sum_{k=0}^{N-1} R_{xx}^k\cos(\omega k\Delta)\right], \tag{28}$$

since $\omega=2\pi m/N\Delta$, the APSD becomes

$$G_{xx}(m)=4\left[R_{xx}^0+\sum_{k=0}^{N-1} R_{xx}^k\cos(2\pi mk/N)\right], \tag{29}$$

where $m=0, 1, \ldots, N/2$.

Because the cross-correlation function is not symmetric, the cross-power spectral density will be a complex quantity. The one-sided CPSD is defined as

$$G_{xy}(\omega)=2\int_{-\infty}^{\infty} R_{xy}(\tau)\,\mathrm{e}^{-j\omega\tau}\,\mathrm{d}\tau, \tag{30}$$

for $0<\omega\leqslant\infty$ (Uhrig, 1970; Bendat and Piersol, 1971). The cross-power spectral density can be written as a real part and an imaginary part

$$G_{xy}(\omega)=C_{xy}(\omega)-jQ_{xy}(\omega), \tag{31}$$

where C_{xy} is termed the co-spectra, and Q_{xy} is termed the quad-spectra (Oppenheim and Schafer, 1989). The derivations of the expressions for the co-spectra and the quad-spectra are given by Uhrig (1970) and are presented here for completeness. First, the integral in equation (31) is separated into two integrals to yield

$$G_{xy}(\omega)=2\int_{-\infty}^{0} R_{xy}(\tau)\,\mathrm{e}^{-j\omega\tau}\,\mathrm{d}\tau+2\int_0^{\infty} R_{xy}(\tau)\,\mathrm{e}^{-j\omega\tau}\,\mathrm{d}\tau. \tag{32}$$

A change of variable is performed in the first integral in equation (32) by setting $\tau=-\tau$ and using the

asymmetry property of the cross-correlation function, $R_{xy}(-\tau)=R_{yx}(\tau)$ to obtain

$$G_{xy}(\omega)=2\int_0^\infty R_{yx}(\tau)\,e^{j\omega\tau}\,d\tau + 2\int_0^\infty R_{xy}(\tau)\,e^{-j\omega\tau}\,d\tau. \quad (33)$$

By substituting Euler's formula into equation (33) and grouping the real and imaginary parts, the following expressions are obtained for the co-spectra and the quad-spectra

$$C_{xy}(\omega)=2\int_0^\infty [R_{xy}(\tau)+R_{yx}(\tau)]\cos(\omega\tau)\,d\tau \quad (34)$$

and

$$Q_{xy}(\omega)=2\int_0^\infty [R_{xy}(\tau)-R_{yx}(\tau)]\sin(\omega\tau)\,d\tau. \quad (35)$$

The cross-correlation functions can be expressed as sequences of discrete samples

$$R_{xy}(\tau)=\sum_{k=0}^{N-1} R_{xy}^k\delta(\tau-k\Delta) \quad (36)$$

and

$$R_{yx}(\tau)=\sum_{k=0}^{N-1} R_{yx}^k(\tau-k\Delta). \quad (37)$$

Substitution of equations (36) and (37) into equations (34) and (35) and rearranging and evaluating the integrals yield the following expressions for the co-spectra and the quad-spectra:

$$C_{xy}(m)=2\left[\sum_{k=0}^{N-1} R_{xy}^k\cos(2\pi mk/N)+\sum_{k=0}^{N-1} R_{yx}^k\cos(2\pi mk/N)\right] \quad (38)$$

and

$$Q_{xy}(m)=2\left[\sum_{k=1}^{N-1} R_{xy}^k\sin(2\pi mk/N)-\sum_{k=1}^{N-1} R_{yx}^k\sin(2\pi mk/N)\right], \quad (39)$$

where the frequency variable has been discretized. These estimates of the APSDs and the CPSDs are then used to calculate the coherence functions and the ratio of spectral densities.

3.5.3. Time domain analysis. Since the code stores the time of particle detections, the time distribution of counts after ^{252}Cf fission can easily be obtained. The birth time of particles from the spontaneous fission of ^{252}Cf is set equal to zero to obtain the detector response after ^{252}Cf fission. The time response calculations are used to benchmark these calculational algorithms for simple configurations measured in the time domain.

3.6. Modified MCNP structure

The general structure of MCNP has been preserved as much as possible. However, some modifications had to be made in order to obtain the frequency data in a manner similar to the measurement. The general flow of MCNP4A is shown in Fig. 2. The program starts by reading the command line to determine which options the code uses. After determining the options, the program begins execution. The first step is to read the input file, which can be stated on the command line or the default input file name, INP. The arrays are initialized with a call to subroutine IMCN. If the frequency analysis calculation is to be performed, a separate data file containing options used in the noise calculation is read in IMCN. After initializing the arrays, the interactive geometry plot subroutine PLOTG is called if the command line contains IP and the options to plot the geometry. Next, the cross section data are read into the appropriate arrays. Once the cross-section data have been placed in the arrays, the code begins the actual tracking of the particles by calling subroutine MCRUN. Subroutine MCRUN runs the particle histories by calling TRNSPT, which, in turn, calls HSTORY to follow the particle tracks throughout the system, and writes the detector information. Finally, the tallies are plotted with a call to MCPLOT after all the particles have been analysed. This general structure has been maintained in the modified code. The major difference occurs in the

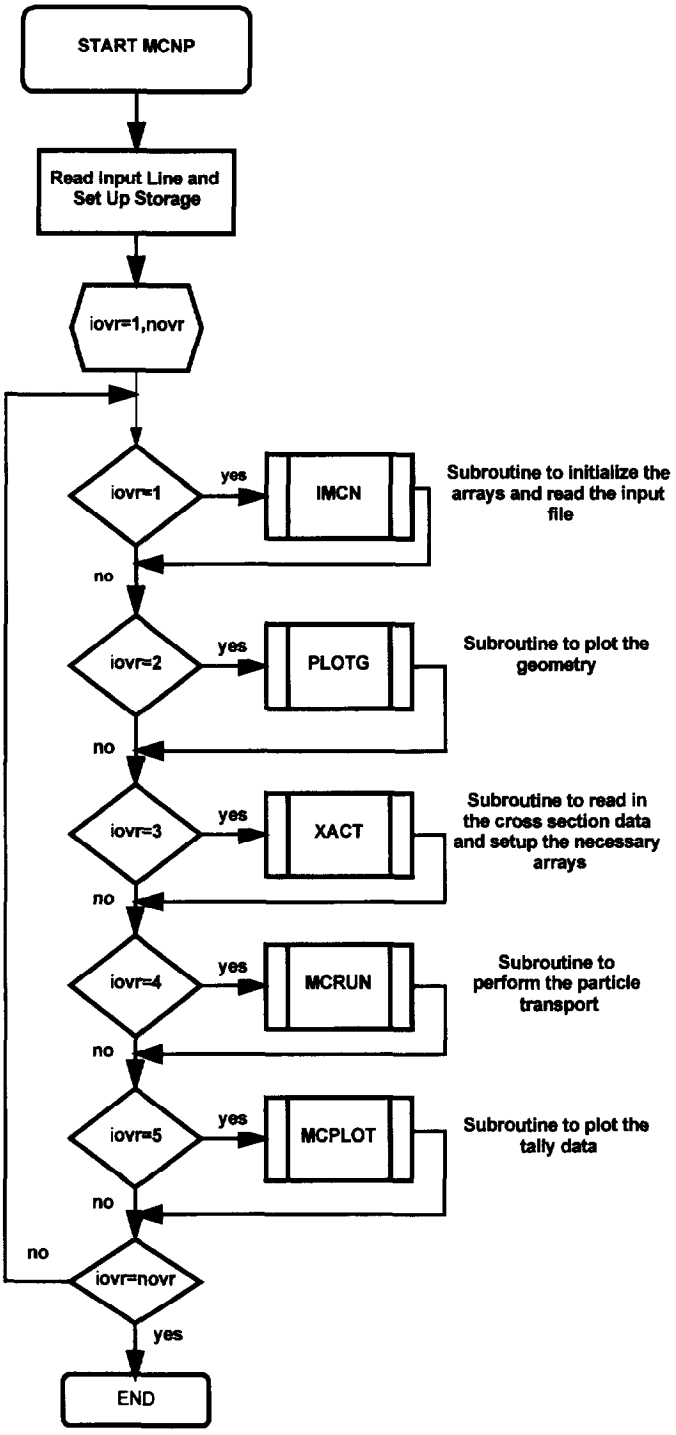
START MCNP
Read Input Line and Set Up Storage
iovr=1,novr
iovr=1
yes
IMCN
Subroutine to initialize the arrays and read the input file
no
iovr=2
yes
PLOTG
Subroutine to plot the geometry
no
iovr=3
yes
XACT
Subroutine to read in the cross section data and setup the necessary arrays
no
iovr=4
yes
MCRUN
Subroutine to perform the particle transport
no
iovr=5
yes
MCPLOT
Subroutine to plot the tally data
no
no
iovr=novr
yes
END

Fig. 2.

actual transporting of the particles. The subroutine TRNSPT has been modified to call HSTORYCF if the noise calculation is to be performed.

The structure of the noise calculation is based on an outer and an inner loop. The outer loop controls the number of blocks of data (*bks*) to be calculated. The average number of source events per data block (*scd*) controls the inner loop. If the inherent spontaneous fission source option is invoked, there is a second inner loop that is controlled by the average number of inherent spontaneous fissions per block (*sfpd*). Because spontaneous fission is a Poisson process, the number of disintegrations per block (*ncdis*) is calculated from a Poisson distribution with mean *scd* for the source events per block and with mean *sfpd* for the inherent fission source fissions per block. The ratio of the ^{252}Cf source fission rate to the inherent source fission rate must be known to specify *scd* and *sfpd*. Detected particles from induced fission caused by the inherent source neutrons contribute correlated information to G_{23} but also contribute uncorrelated information to G_{12} and G_{13}. The average number of source events per data block is related to the actual source size by the following relation (Ficaro, 1991)

$$scd=\frac{mR_{sf}ntbn}{f_s}, \tag{40}$$

where m is the mass of the source in micrograms, R_{sf} is the spontaneous fission rate of the source per microgram, *ntbn* is the number of points per block, and f_s is the sampling rate. Using this expression, the source specified in the calculation can be related to the actual source used in the measurements. For calculations employing the inherent fission source option, it has been shown that it is not necessary to use the actual R_{sf} but only maintain the ratio of *scd* and *sfpb*. The particle tracking begins with the first data block. First, the source particles and their progeny are tracked. Next, the particles from the inherent fission source and their progeny are tracked if this option is invoked. When the inner loops are finished, the block data are processed. This processing could be the direct calculation of the power spectral densities or the calculation of the correlation functions. After the block data have been processed, the outer loop variable is incremented and the inner loops are restarted. When all of the data blocks have been calculated, the outer loop is completed. The summary information is written to the output files, and if the data were processed in the correlation function mode, the power spectral densities are calculated and written to a file. This process is depicted in Fig. 3.

Since the inner loops control the actual particle transport, a detailed description of the particle tracking follows. The inner loop begins by obtaining information about the source particles. The position is specified in the extra data file for the source particles and is chosen randomly in a specified volume for the inherent fission source. The time of the spontaneous fission is chosen randomly in the data block. The number of particles from the source is chosen randomly. Spencer's distribution is used to obtain the number of prompt neutrons from the ^{252}Cf source, and Brunson's distribution is used to determine the number of prompt gamma rays from the ^{252}Cf source. Terrell's formula is used to determine the number of prompt neutrons from the inherent spontaneous fission source. The energies of the ^{252}Cf neutrons are chosen from the corrected Maxwellian distribution, and the energies of the ^{252}Cf gamma rays are chosen from Maienschein's spectrum. The energy spectra of the inherent fission source neutrons are chosen from the usual MCNP Watt fission spectrum. The direction of the source neutrons can be chosen isotropically or from the angular distribution data of Budtz-Jorgensen and Knitter. All but one of the particles are stored in the bank. An overview of the particle tracking is shown schematically in Fig. 4. The distance to the cell boundary, d_b, is determined from the particle's starting location and the direction cosines. Next, the distance to the collision site, d_c, is calculated from the usual relation $d_c=-\ln R/\Sigma_t$, where R is a random number and Σ_t is the total macroscopic cross section. The minimum distance determines whether or not the particle has a collision. If d_b is less than d_c, the particle is transported through the cell boundary, where the distance to the next cell boundary and the distance to collision is calculated for the new cell. If the particle enters a region of zero importance (outside the system), the particle is said to have leaked, and the leakage tallies are updated. If the d_c is less than d_b, then the particle collides in the cell. When a particle collides, the collision nuclide is selected randomly from the materials present in the cell. If the particle is a neutron, the velocity of the collision nuclide is calculated, and the collision event is determined. The capture probability is calculated in the usual way. If the problem is a dual neutron–gamma ray calculation, gamma rays may be produced by the neutron interaction. If the particle is not lost by capture, the neutron will have either an elastic collision, or an inelastic collision.† The probability of having an elastic collision is given by $\sigma_{el}/(\sigma_{el}+\sigma_{in})$ where σ_{el} is the microscopic elastic scattering cross section, and

† The term inelastic collision is a carryover from MCNP and means all reaction except elastic scattering and capture.

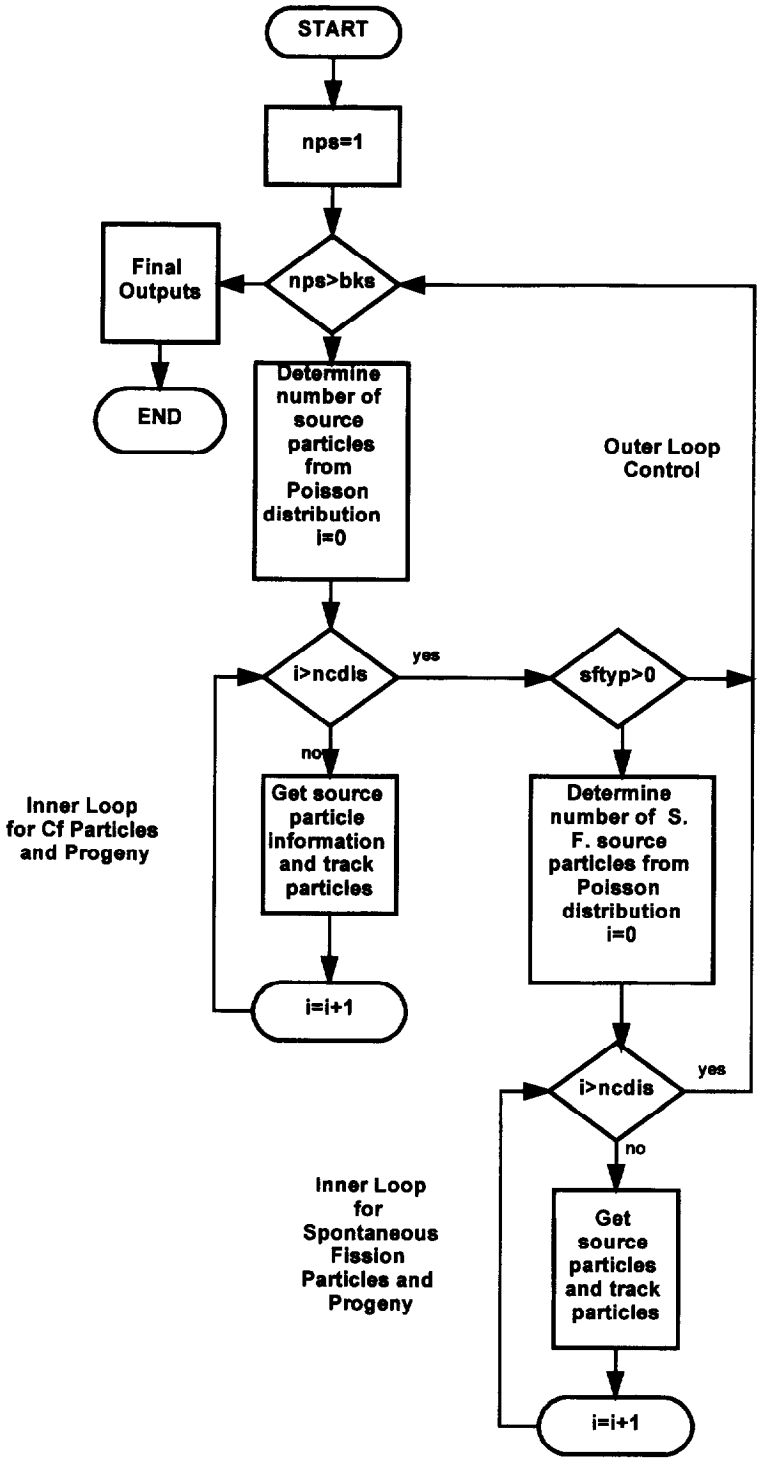
START
nps=1
Final Outputs
nps>bks
END
Determine number of source particles from Poisson distribution i=0
Outer Loop Control
i>ncdis
yes
sftyp>0
no
Get source particle information and track particles
Determine number of S. F. source particles from Poisson distribution i=0
Inner Loop for Cf Particles and Progeny
i=i+1
i>ncdis
yes
no
Inner Loop for Spontaneous Fission Particles and Progeny
Get source particles and track particles
i=i+1

Fig. 3.

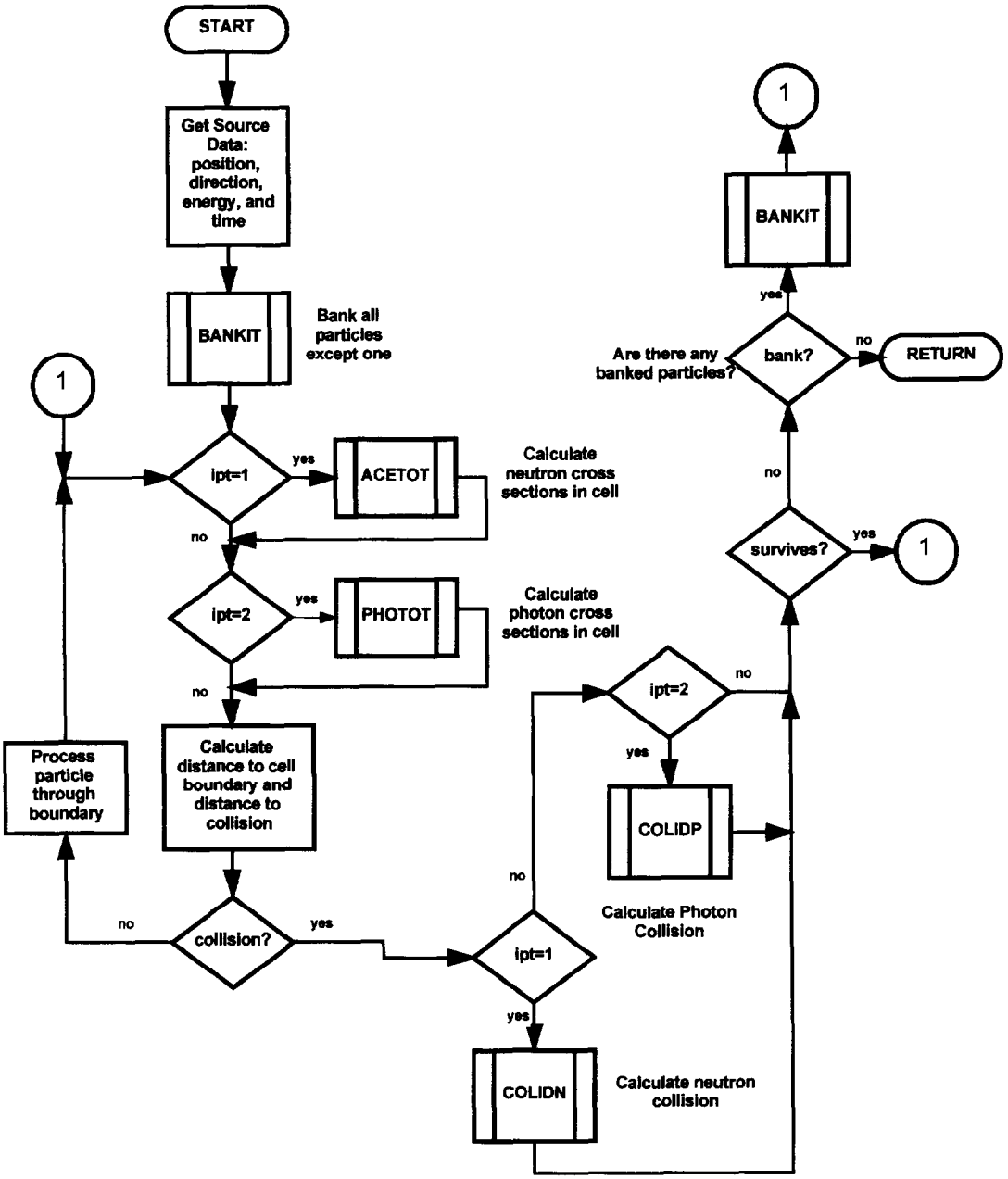

Fig. 4.

σ_{in} is the microscopic inelastic cross section. The type of inelastic event, n, is determined from

$$\sum_{i=1}^{n-1} \sigma_i < \xi \sum_{i=1}^{N} \sigma_i \leqslant \sum_{i=1}^{n} \sigma_i, \tag{41}$$

where ξ is a random number on the interval [0 to 1), N is the number of inelastic reactions, and the σ_is are the inelastic reaction cross sections at the incident neutron energy (Briesmeister, 1993). If the inelastic event is fission, the number of neutrons produced from fission is determined from Zucker and Holden's data or from Terrell's formula, depending on the fissioning isotope. The energy of the emerging

neutrons is sampled from the appropriate spectrum indicated in the cross-section data file. The direction cosines may be either isotropic or determined from the experimental angular distribution data. Any neutrons produced from fission are banked to be tracked later.

If the particle is a gamma ray, the determination of the type of interaction is the same as that used for neutron collisions. However, the collision physics are different (Briesmeister, 1993). In the modified code the detailed physics treatment is used by default. The detailed physics treatment includes incoherent scattering, coherent scattering, the photoelectric effect, and pair production. Therefore, the total gamma ray cross section, σ_t, is

$$\sigma_t = \sigma_{IC} + \sigma_{CO} + \sigma_{pe} + \sigma_{pp}, \tag{42}$$

where σ_{IC} is the incoherent scattering cross section, σ_{CO} is the coherent scattering cross section, σ_{pe} is the photoelectric cross section, and σ_{pp} is the pair production cross section. The selection of the gamma ray event is determined in a similar manner to the neutron events.

The tracking and collision process is repeated for each particle until the particle either leaves from the system or is absorbed by analog capture. Next, particles are retrieved from the bank, and the tracking process proceeds as before until all the source particles and their progeny have been tracked for the given data block. Then, the particles for the inherent fission source are tracked if the spontaneous fission source option is invoked. The inner loops are now complete for one data block, and the detector responses are then processed. After processing the detector responses, the outer loop variable is incremented, and the inner loop procedure is repeated. After the desired number of blocks has been calculated, the program calculates the final estimates of the APSDs and CPSDs and writes the data to a file.

4. CONCLUSIONS

MCNP-DSP was developed in order to calculate the ratio of spectral densities $R(\omega)$, other frequency analysis parameters (APSDs and CPSDs), time analysis quantities such as autocorrelation and cross-correlation functions, and the time distribution of counts after ^{252}Cf fission using the Monte Carlo technique. This work was undertaken to provide a more general method of calculating time and frequency analyses measured parameters than KENO-NR which is a neutron only code with group cross sections. MCNP-DSP time correlates both the neutrons and gamma rays from fission and provides a more general model for interpretation of subcriticality measurements that does not suffer from the inadequacies of the point kinetics model. To perform these calculations of the measured data, several modifications were included in MCNP-DSP. The structure of the code was modified in order to obtain the detector responses in the form of data blocks, as in the measurements. The weighting and biasing in MCNP are disabled in order to have a strictly analog Monte Carlo calculation. A dual particle source was developed which produces both time correlated neutrons and gamma rays from the spontaneous fission of ^{252}Cf. An option for including a distributed inherent fission source is also incorporated. Evaluated measured neutron and gamma ray data are also incorporated into the code for certain neutron and gamma ray interactions. A simplified detector scattering treatment is included in MCNP-DSP. Detector processing algorithms are incorporated into the code to process the data blocks of the detector responses in the same way as a measurement. The frequency spectra are obtained by direct Fourier processing of the blocks of data to obtain the APSDs and CPSDs or by Fourier transforming the autocorrelation and cross-correlation functions.

MCNP-DSP provides a more general continuous energy Monte Carlo model for calculation of measured observables which includes not only neutrons but also gamma rays. This code can be used to calculate frequency analysis parameters for in-plant configurations of fissile material. MCNP-DSP can be used to validate calculational methods and cross section data sets with measured data from subcritical experiments. In most cases the frequency analysis parameters are more sensitive to cross section changes by as much as 1 or 2 orders of magnitude and then may be more useful than comparisons of neutron multiplication factor for calculational validation. The use of MCNP-DSP model in place of a point kinetics model to interpret subcritical experiments extends the usefulness of this measurement method to systems with much lower neutron multiplication factors. MCNP-DSP can also be used to determine the calculational bias in the neutron multiplication factor (a quantity which is essential to the criticality safety specialist) from in-plant subcritical experiments. MCNP-DSP provides a more general tool for planning and interpreting experiments for criticality safety, safeguards, nondestructive assay, and arms control verification.

Acknowledgements—The authors are grateful to R. A. Forster, R. Seamon, G. W. McKinney, and J. R. Nix of Los Alamos National Laboratory for their consultation during this work.

REFERENCES

Bendat J. S. and Piersol A. G. (1971) *Random Data: Analysis and Measurement Procedures*. Wiley, New York.

Briesmeister J. F., Ed. (1993) La-12625-M, Los Alamos National Laboratory.

Brunson G. S. Jr. (1982) Ph.D Thesis, Univ. of Utah.

Budtz-Jorgensen C. and Knitter H. H. (1988) *Nucl. Phys.* **A490,** 307.

Ficaro E. P. (1991) Ph.D Dissertation, Univ. of Michigan.

Goldstein H. (1959) *Fundamental Aspects of Reactor Shielding*. Addison-Wesley, Reading, MA.

Jankowski F. J., Klein D. and Miller T. M. (1957) *Nucl. Sci. Eng.* **2,** 288.

King W. T. (1980) Ph.D Dissertation, Univ. of Tennessee.

Maienschein F. C., Peelle R. W. and Love T. A. (1958) *Neutron Phys. Ann. Prog. Rep. Sept. 1*, ORNL-2609, Oak Ridge National Laboratory.

Mannhart W. (1987) *Proc. Advisory Group Mtg. Neutron Sources*, Leningrad, U.S.S.R., 1986, IAEA-TECDOC-410, Vienna.

Mihalczo J. T. (1971) *Nuc. Sci. Eng.* **46**, 147.

Mihalczo J. T. (1974) *Nucl. Sci. Eng.* **53**, 393–414.

Mihalczo J. T. and Paré V. K. (1994) Arms Control and Nonproliferation Technologies, DOE/AN/ACT-94C (Third Quarter 94).

Milhalczo J. T., Paré V. K., Ragen G. L., Mathis M. V. and Tillet G. C. (1978) 'Determination of Reactivity from Power Spectral Density Measurements with Californium-252', *Nucl. Sci. Eng.* **66**, 29–59.

Mihalczo J. T. and Valentine T. E. (1995) *The Fifth Int. Conf. on Nuclear Criticality Safety*, Albuquerque, New Mexico, September.

Mihalczo J. T. and Valentine T. E. (1995) *Nucl. Sci. Eng.* **121,** 2.

Mihalczo J. T., Valentine T. E. and Phillips L. D. (1995a) *The Fifth Int. Conf. on Nuclear Criticality Safety*, Albuquerque, New Mexico, September.

Mihalczo J. T., Paré V. K., Turner G. W. and Fisher J. R. (1995b) *INMM*, 36th Annual Meeting, Palm Desert, Calif., July.

Mueller R. E., Nicholson R. B. and Zweifel P. F. (1962) *Trans. Am. Nucl. Soc.* **5,** 67.

Nifenecker H., Signarbieux C., Ribrag M., Poitou J. and Matuszek J. (1972) *Nucl. Phys.* **A189,** 209.

Nix J. R. (1994) Personal communication.

Oppenheim A. V. and Schafer R. W. (1989) *Discrete-Time Signal Processing*. Prentice-Hall, Englewood Cliffs, NJ.

Orndoff J. D. (1957) *Nucl. Sci. Eng.* **2,** 450.

Paré V. K. and Mihalczo J. T. (1975) *Nucl. Sci. Eng.* **56,** 213.

Petrie L. M. and Landers N. F. (1984) ORNL/NUREG/CSD-2, Oak Ridge National Laboratory.

Ricker C. W., Fry D. N., Mann E. R. and Hanauer S. H. (1963) *Proc. of the Symposium on Noise Analysis in Nuclear Systems*, Univ. of Florida.

Sastre C. A. (1960) *Nucl. Sci. Eng.* **8,** 443.

Seamon R. (1994) Personal communication.

Simmons B. E. and King J. S. (1958) *Nucl. Sci. Eng.* **3,** 595.

Spencer R. R., Gwin R. and Ingle R. (1982) *Nucl. Sci. Eng.* **80,** 603.

Terrel, J. (1959) *Phys Rev.* **113**, 527.

Uhrig R. E. (1970) *Random Noise Techniques in Nuclear Reactor Systems*. The Ronald Press Company, New York.

Vandenbosch R. and Huizenga J. R. (1973) *Nuclear Fission*. Academic Press, New York.

Wagemans C. (1991) *The Nuclear Fission Process*. CRC Press, Boca Raton, FL.

Zucker M. S. and Holden N. E. (1986) *Trans. Am. Nucl. Soc.* **52,** 630.